International Journal of Energy Engineering 2013, 3(5): 242-255
DOI: 10.5923/j.ijee.20130305.03

High Velocity Impact Response Evaluation of a Glass Fibre Reinforced Polymer (GFRP) Composite - Amour Body

Onyechi Pius C.[1], Edelugo Sylvester O.[2], Ihueze Chukwutoo C.[1], Obuka Nnaemeka S. P.[3,*], Chukwumuanya Okechukwu E.[1]

[1]Department of Industrial and Production Engineering, Nnamdi Azikiwe University, Awka, Nigeria
[2]Department of Mechanical Engineering, University of Nigeria, Nsukka, Nigeria
[3]Department Mechanical and Production Engineering, Enugu State University of Science and Technology, Enugu, Nigeria

Abstract Impact on composites is a very complex phenomenon and function of many parameters influencing its analysis. This research developed an armour protecting body of Glass Fibre Reinforced Polyester (GFRP) composite laminates of varying thicknesses of 8mm, 12mm, 16mm, 20mm, 24mm, and 28mm. the impact response of these composites was investigated. The impact resistance and subsequent load-bearing capacity of the composites depend on many factors such as; fibre and matrix properties, fibre-matrix lay-up, number of layers or ply, thickness and impact velocity. These GFRP composites were targeted with a high velocity of 355m/s, using two types of life bullets (Ogival and Conical nosed). The developed composite armour proved considerable strength of 145.83MPa before ballistic deformation and 97.3MPa after ballistic deformation. Ballistic impact tests show that 5Samples out of the 6 Samples produced were able to withstand the impact velocity of the bullets, with Sample E showing a complete absorption of the bullet, while Sample F was perforated.

Keywords GFRP Composite, Armour Body, Impact Velocity, Ogival Nosed, Conical Nosed, Ballistic Impact

1. Introduction

Glass Fibre Reinforced Plastic (GFRP) automobile, ships, aeroplanes, and armoured vehicle bodies production offers Nigerians an appropriate technology. The problems of heavy initial capital investment on high-temperature furnaces and heavy press with complex dies without their maintenance technology are very significant. GFRP production is very cheap and do not require skilled manpower.

However, a major concern about the use of the composite is their low resistance to out-of-plane localized impact loading. A number of works have been reported in the fields of impact phenomenon of fibre reinforced composites materials. Especially, the damage resistance and damage tolerance under impact loading are of the most importance of composite material characteristics because they are often susceptible to impact. Impact on composites is a very complex phenomenon and function of many parameters influencing its analysis. The advanced composites materials are being looked upon as the key materials for applications in armoured vehicle technology, automobile, ship, aerospace industries and ballistic protection. The design of composite armour is a very complex task as compared to conventional single-layer metallic armour, due to the exhibition of coupling among membrane, torsion and bending strains, weak transverse shear strength and discontinuity of the mechanical properties along the thickness of the composite laminates. This has drawn attention of several researchers to study the penetration phenomenon in composite amours.

The impact resistance and subsequent load-bearing capacity of composite depend on many factors such as fibre and matrix properties, fibre-matrix lay-up, number of layers or ply, thickness, and impact velocity. Cantwell et al (1989) and Prewo (1980) stated that the impact, resulting in complete penetration of laminate due to the high velocity is called ballistic impact and is of major concern to the armour designers. Further, the damage caused to the armour under high velocity impact is quite significant and has major effects on the dynamic properties of the laminates.

2. Literature Review

2.1. Properties of Glass Reinforced Plastics

The outstanding properties of composite materials led to products that are superior and competitive in the international markets. The glass-fibre reinforcement comes

* Corresponding author:
silvermeks7777@yahoo.com (Obuka Nnaemeka S.P.)
Published online at http://journal.sapub.org/ijee
Copyright © 2013 Scientific & Academic Publishing. All Rights Reserved

in a number of forms including roving, woven glass cloth and Glass mats[3]. Glass-fibre is the most common reinforcement used in polymeric composite formulation use in aerospace, aircraft, military and ballistic protection. Reinforcement plays a dominant role determining mechanical strength properties of composite. The primary reinforcement includes Glass-fibre or Fibre glass, Graphite and Aramid (Kevlar).

The two main components of a GRP composite are the matrix and the reinforcing glass. The matrix is the continuous phase. In itself, the matrix does not provide strength, its role is essential, however, since it serves to bond the reinforcing glass-fibre together and to transfer the load to the reinforcing phase. The glass content of GRP composites effects strength properties and durability (the higher the glass-fibre content, the stronger the material). However, too high a glass content may result to insufficient impregnation, and therefore poorer bonding. The glass content of GRP reinforced with chopped strand mat generally varies between 25 to 35 %; for GRP reinforced with cloth, the glass content ranges from 50 to 63 %. Sheet material manufactured by hand lay-up process will have lower strength properties than those fabricated by a press-molding process.

The range of mechanical and other physical properties is very wide, because of the great number of factors which define a GFRP composite. For example, the tensile strength at room temperature may vary from 69 MPa to 896 MPa or higher, wet strength retention from 50 to 95 % and specific gravity from 1.2 to 1.9. The range of some physical properties is given in Table 1. They are typical for GFRP sheet materials produced with normal care from general purpose polyester resin and reinforced with three types of glass-fibre reinforcement. More complete data on physical properties of GFRP composite can be found in reference [4],[5] and[6].

The comparative average mechanical properties of high performance fibre laminates can be found in Table 2.

Also, the thickness of the component laminate is the single most important factor to determine a moulding as it affects directly the quantity of re-enforcement and resin. Table 3 shows the number of plies of laminate in hand lay-up for a given average thickness of laminate.

Table 1. Physical Properties of Glass-fibre Reinforced Polyester Sheet reinforced with various glass fibre constructions[7] and[8]

Property*	Type of Reinforcement		
	Chopped-Strand Mat or Premix**	Parallel Roving	143 Fabric Parallel Laminated
Glass Content, (by weight, %)	25 – 45	50 – 70	62 – 67
Specific Gravity	1.4 – 1.6	1.7 – 1.9	1.7 – 1.9
Tensile Strength, MPa (10^3 psi)	76 – 160 11 – 23	550 – 900 80 – 130	540 – 600 78 – 87
Tensile Modulus, MPa (10^3 psi)	5.6 – 12 0.82 – 1.8	– –	31 4.5
Flexural Strength, MPa (10^3 psi)	140 – 260 20 – 38	690 – 1400 100 – 2-00	590 – 720 85 – 105
Flexural Modulus, MPa (10^6 psi)	6.9 – 14 1.0 – 2.0	34 – 49 5.0 – 7.0	31 – 38 4.5 – 5.5
Compressive Strength, Mpa (10^3 psi)	120 – 180 189 – 26	340 – 480 50 – 70	280 – 340 40 – 50

* The matrix is based on general purpose unsaturated thermosetting polyester resin.
** Resistance to continuous heat (150 – 205^{0}C; 300 – 400^{0}F), (Agrannoff, 1975).

Table 2. Comparative Average Mechanical Properties of High Performance Fibre Laminates

Parameter/Quantity	Fiber Glass	Kevlar- 49	Spectra 1000
Laminate thickness (mm)	6.35	6.35	0.41
Density (kg/m^3)	2000	1260	970
Tensile Strength, s (MPa)	344.50	337.60	1034.00
Tensile Modulus, E (GPa)	20.67	13.10	50.03
Flexural Strength (MPa)	137.80	49.60	158.50
Flexural Modulus (GPa)	17.20	3.45	22.74
Compressive Strength (MPa)	75.79	33.76	72.35
Specific Strength (s/r)	1.723E+05	2.679E+05	1.066E+06
Specific Modulus (E/r)	1.034E+07	1.040+07	5.158E+07
Water Absorption (%)	0.75	2.50	< 0.10
Fiber Glass In Polyester; Kevlar In Polyester, Phenol, Vinyl Ester; Spectra In Epoxy (Babaniyi, 2000).			

Table 3. Hand Lay-Up, Average Thickness in mm per number of Plies (Courtesy Owens Corning Fibreglass) [9]

Laminate	Number of Plies														
	1	2	3	4	5	6	7	8	9	10	11	12	13	14	15
2 oz mat (57g)	1.5	2.8	4.5	6.0	7.5	9.5	10.75	12.5	13.5	15.5	17.0	18.75	20.25	22.0	23.0
24 oz woven roving (680g)	0.93	1.7	2.5	3.6	4.7	6.0	6.5	7.6	8.5	9.5	10.5	11.5	12.4	13.3	14.3
10 oz cloth (280g)	0.4	0.78	1.2	1.6	2.0	2.4	2.8	3.2	3.6	4.0	4.4	5.0	5.3	5.7	6.2
Fabmat 2415	2.0	3.8	5.6	7.6	9.5	10.5	12.7	14.5	16.5	18.4	20.3	22.2	24.1	32.0	34

2.2. Review of Related Works

Since 1950, fibre-reinforced composites have been used in wide variety of industries. Industries as diverse as transportation, construction, marine, offshore oil, sporting goods have recognized those benefits and are extensively making use of these materials. Enetanya (1998) investigated the fibre- reinforced composite for the aircraft and automobile industries on a paper presented at a technical sessions of the Nigerian Society of Engineers. Edelugo (2000) worked on reinforcement combination for GRP in Auto-body works while[12] investigated the influence of the fibre reinforcement combination on the buckling failure of GFRP composites.

Ballistic type of impact tests were studied by Europeans in an attempt to study speed effects of a projectile that would maximize the damage. The study of foreign objects became critical for speed and shape of indenters relationship. The first ballistic impact resistance test was conducted on the GRP in 1940. In their study it was found that the maximum de-lamination damaged area was a linear function of the force of impact whether the force was introduced by falling weight or static indentation tests. As impact testing of composite laminates becoming routine and matured, test methods and analyses have become well defined. In particular instrumented impact on non-catastrophic testing is being widely used where impact analyses have been broken down into dynamic response and quasi static response[13] and[14].

The analysis of high velocity impact problems has been of interest for many years. Solution to these problems often require the inclusion of large strains and displacement, as well as the materials strength and compressibility effects, the analysis techniques are complicated and large computer codes are necessary to obtain these solutions. The earlier solutions of high velocity impact problems were often obtained with two-dimensional Lagrangian codes such as HEMP by Wilkin and TOODY II by[15]. Two-dimensional Eulerian codes such as HELP program by[16] were later applied to these problems. A three-dimensional version of HEMP has also been developed[17]. The finite-element method has recently been applied to two-dimensional impact problems involving severe distortion[18]. A comprehensive description of various finite-element methods is given in references works by[19] and[20]. The work presented herein is an extension of that presented in[18] with the technique being extended for axisymmetric, two-dimensional, triangular elements to three-dimensional tetrahedron elements,[21]. Various theories proposed for predicting the characteristics of penetration of composite laminates by different projectiles have been reviewed by[20], and[21].

The impact response and damage mechanism are very complex and depend on a number of parameters such as impact velocity, impact energy, impact angle. During high velocity impact by projectiles, the target response is controlled by the local behavior of the materials because of the relatively small impact mass and short contact duration. Therefore the available kinetic energy is usually dissipated over a small zone surrounding the contact area and the failure mode is dominated by perforation. High velocity projectiles owe their destructive penetrating ability to the kinetic energy they carry with them. Conversely, the efficacy of any material resisting such kinetic energy projectiles depends on its ability to absorb the kinetic energy. The energy absorption capacity in turn depends on target material properties. For a given set of properties of laminate targets, the absorption capability also depends on the anisotropic nature of the target material, the thickness of the target, the angle of attack and the type of projectile. Kumar and Bhart (1998) studied the effect of thickness of the laminates and the angle of attack on the energy absorption by the composite laminates and the area of damage caused by impact. Wen H.M et al (2001) and He et al. (2006) presented analytical equation for the prediction of the penetration and perforation of thick FRP laminates struck normally by missiles over a range of impact velocities.

A variety of numerical techniques have been used to study and predict the behavior of composite laminates subjected to impact. Both solid mechanics and fracture mechanics have been used to analyze impact phenomena. In the fracture mechanics approach, change is assumed to occur around an initiated crack due to stress concentrations at the crack tip. Therefore, decision must be taken where crack initiation has occurred and model local crack growth phenomena. In solid mechanics approach, fracture and local phenomena are averaged to model global structural behaviours. Damage is predicted when values of the stress or strain field satisfy a failure criterion. A solid mechanics approach will be taken for this analysis to model global processes rather than treating local phenomena such as fibre/matrix interation and inter-lamina boundary effects. There are many examples in the literature of analytical treatment of impact on composite.

To study the influence of various parameters affecting the penetration process in high velocity impact, the model should be able to describe the physical events, such as indentation, fibre breakage, de-lamination, bulging occurring during penetration.

3. Materials and Applicable Methods

3.1. Experimental Procedure

The class of glass fibres used in this work is the matted woven roving E-glass procured from NYCIL Chemical Industries Nkpor, Idemili North L.G.A., Anambra State, Nigeria. E-glass class, which is a low alkali Borosilicate was initially, developed for electrical application, hence the designation E. The diameter of each E-glass fibre is about 0.01 mm with an average length of 50mm. It has a density of 2550kg/m^3; Young's Modulus of 72 GN/m^3; and a strength of roughly 3.4 GN/m^2. The Polyester Resin used for this work was also procured from NYCIL. It services as the polymer matrix (greatest in percentage of the reagents) for the sample preparation. The speed at which the resin sets can be controlled by the quantity of catalyst and accelerator used.

Methyl Ethyl Ketone Peroxide (MEKP), served as catalyst to the reaction process. Cobalt II Ethyl Hexanoate acted as an accelerator for the release of the free of radical that enhances curing by the catalyst. Paraffin Wax was applied on the surface of mould to enhance the ease removal of the prepared sample from the mould untampered. This is also called a releasing agent. The hand lay-up method was used in formation of the composite materials. Here the polyester resin was applied on the mould evenly with the help of a hand brush to a thickness of about 1mm, then the woven roving fibres were lay-up in the mould and properly wetted out in a process known as fibre impregnation. More fibre plies were lay-up in the mould and compressed according to the required laminate thickness. For the thickness of 28 mm, 24 mm, 20 mm, 16 mm, 12mm and 8mm, the number of plies were 22, 18, 15, 12, 9, and 6 respectively. The fibre content by volume fraction varies from 0.48 to 0.50.

3.2. Formulations for Armour Applications (Ballistic)

It is assumed that the mean pressure (σ) applied normally to the surface of the projectile provided by a GFRP laminate material to resist penetration and perforation by the projectile can be decomposed into two parts, one part is resistive pressure (σ_s) due to the elastic-plastic deformations of the laminate material and the other is the dynamic resistive pressure (σ_d) arising from velocity effects. Thus;

$$\sigma = \sigma_s + \sigma_d \quad (1)$$

If it is further assumed that resistive pressure is equal to static linear elastic limit (σ_e) in through-thickness compression of the GFRP laminates[17];[18], that is $\sigma_s = \sigma_e$ and that the dynamic resistive pressure (σ_d) which is a function of the parameter., $(\rho_t/\sigma_e)^{0.5}V_i$ and is taken to be $\sigma_d = \beta\left((\rho_t/\sigma_e)\right)^{0.5} V_i\sigma_e$, then equation (1) can be written as

$$\sigma = \left[1 + \beta\left(\frac{\rho_t}{\sigma_e}\right)^{0.5} V_i\right]\sigma_e \quad (2)$$

Where ρ_t and V_i are the density of the GFRP laminate and the initial impact velocity of the projectile respectively. The values of the term β were easily determined experimentally for simple geometries. For a unidirectional laminate β=1, while for a (0/90) cross-piled laminate with equal proportions of the fibre in the two direction β= 0.5. For a (±45, 90) composite with one quarter of the fibres in each direction β= 0.375. For a three dimensional random array β= 0.2[11]. Also, the values of the parameter β in the equations have been empirically determined and are taken to be equal to $2\,Sin(\theta/2)\ and\ 3/4\psi$ for conical-nosed and ogival - nosed projectiles respectively[25]. For fibre-reinforced plastic it has been observed in the static indentation tests[26] that the first term in equation (2) is related to the static strength of FRP laminates in compression in the two principal directions, through the thickness and in-plane. Abdulla and Cantwell (2006) used equation (2) to predict the ballistic limit of fibre-metal laminates. The same assumption (eqn. 2) was used by [28] in their study of the penetration of fibre-reinforced plastic.

3.2.1. Penetration of Semi-Infinite GFRP Laminates

The types of projectiles (life bullets) that were used are the rigid projectile with ogival and conical nosed.

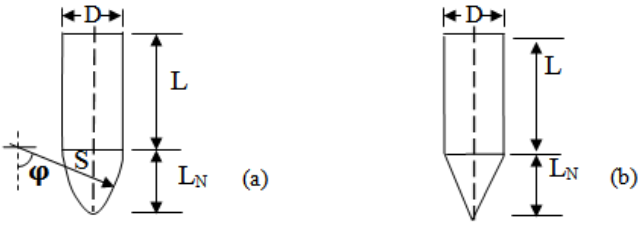

Figure 1. Projectile geometries (a) Ogival nose and (b) Conical nose

The projectiles are assumed to have density ρ_p and mass M with diameter D (or radius r), L and L_N are the lengths of the shank and nose of ogival and conical projectile as shown in Fig 1. Fig 1(a) shows the ogive profile as the arc of the circle(s) that is tangent to the shank. It is also common to define the ogive in terms of caliber – radius – head.

Table 4. Classification of Bullets used [29]

Parameter	Ogival	Conical
Projectile Caliber	22 (5.6 mm)	45° conical tipped
Cartridge size Type	27grain	27grain
Nominal Type	1.7gram	1.7gram
Bullet diameter	5.7mm	5.7mm
Velocity	355m/s	355m/s
Effective range	200meters	200meters
Mass Density of Bullet	11,400kg/m^3	11,400kg/m^3

Source: Wikipedia, the free encyclopedia.

3.2.2. Conical-Nosed Projectiles

For a rigid conical-nosed projectile, the motion and the final depth of penetration can be calculated if the resistive forces are known.

(i) Case (i), $d_p \leq L_N$

The resistive force of a conical-nosed projectile penetrating an FRP laminate target at normal incidence can be written as;

$$F = \sigma A \tag{3}$$

Where F is the resistive force and σ is the mean resistive pressure provided by the target material and A, is instant cross-sectional area.

$$A = \pi {d_p}^2 tan^2 \frac{\theta}{2} \tag{4}$$

θ and d_p is the cone angle and the depth of penetration respectively. Substituting equations (2) and (3) in (4) gives;

$$F = \pi {d_p}^2 tan^2 \frac{\theta}{2} \left[1 + \beta \left(\frac{\rho_t}{\sigma_e}\right)^{0.5} V_i\right] \sigma_e \tag{5}$$

For energy conservation, one obtains;

$$E_k = \int_0^{d_p} F d\left(d_p\right) \tag{6}$$

Where E_k; is the initial kinetic energy of the projectile. Substituting equation (5) in (6) will yield.

$$E_k = \frac{{d_p}^3 A_0}{3\,{L_N}^2} \left[1 + \beta \left(\frac{\rho_t}{\sigma_e}\right)^{0.5} V_i\right] \sigma_e \tag{7}$$

Using tan (θ/2) = r/L_N and $A_o = \pi r^2$. Here A_o is the cross-sectional area of the projectile shank.

Substituting $E_k = ½\ m{V_i}^2$ into equation (7) and rearranging gives that, [30].

$$\frac{d_p}{L+\frac{L_N}{3}} = \left(\frac{\rho_p}{\rho_t}\right) \frac{\rho_t {V_i}^2}{\sigma_e} \frac{1}{\frac{2}{3}\left[1+\beta\left(\frac{\rho_t}{\sigma_e}\right)^{0.5} V_i\right]\left(\frac{d_p}{L_N}\right)^2} \tag{8}$$

And $m = A_0 \left(L + \frac{L_N}{3}\right) \rho_p$

Case (ii) $d_p > L_N$

The resistive force F can be written as;

$$F = A_0 \sigma = A_0 \sigma_e \left[1 + \beta \left(\frac{\rho_t}{\sigma_e}\right)^{0.5} V_i\right] \tag{9}$$

According to energy balance, one obtains,

$$E_k = \int_0^{L_N} F d\left(d_p\right) + \int_{L_N}^{p} F d\left(d_p\right) \tag{10}$$

Substituting (5) and (9) in (10) yields;

$$E_k = \left(d_p - \frac{2}{3} L_N\right) A_0\, \sigma_e \left[1 + \beta \left(\frac{\rho_t}{\sigma_e}\right)^{0.5} V_i\right] \tag{11}$$

Substituting $E_k = 1/2\, G {V_i}^2$ into (11) and using $G = A_0(L + L_N/3)\rho_p$ gives the final depth of penetration as;

$$d_p = \left(L + \frac{L_N}{3}\right) \left[\left(\frac{\rho_p}{\rho_t}\right) \frac{\rho_t {V_i}^2}{\sigma_e} \frac{1}{\left[1+\beta\left(\frac{\rho_t}{\sigma_e}\right)^{0.5} V_i\right]} + \frac{2}{3\left(\frac{L}{L_N}\right)+1}\right] \tag{12}$$

3.2.3. Ogival-Nosed Projectiles

(i) Case (i) $d_p < L_N$[31]

$$\rho_p (L + 8\Psi^3 \eta r) V_i^2 = 16\Psi^3 r\, \sigma_e \begin{bmatrix} -\cos\varphi + {}^1\!/_3 \cos^3\varphi - \left(\Psi - {}^1\!/_2 \sin 2\varphi\right) \sin\varphi_0 \\ -\sin^2\varphi_0 \cos\varphi + {}^\pi\!/_2 \sin\varphi_0 + \eta \end{bmatrix} \tag{13}$$

$$d_p = [(4\Psi - 1)^{0.5} - 2\Psi \cos\varphi] r \tag{14}$$

In which φ is the tip angle, r is the radius of the projectile, and the mean resistive pressure **σ** is determined by Eq. (2) $\boldsymbol{\varphi}_o$ and η are evaluated as follows;

$$\varphi_0 = Sin^{-1}\left(\frac{2\psi - 1}{2\psi}\right) \tag{15}$$

(ii) Case (ii) $d_p > L_N$

$$\frac{d_p}{L+8\psi^3\eta\gamma} = \left(\frac{\boldsymbol{\rho_p}}{\boldsymbol{\rho_t}}\right) \frac{\boldsymbol{\rho_t} {V_i}^2}{\sigma_e} \frac{\mathbf{1}}{\mathbf{2}\left[1+\beta\left(\frac{\rho_t}{\sigma_e}\right)^{0.5} V_i\right]} + \frac{[(\mathbf{4}\psi-1)^{\mathbf{0.5}} - 8\psi^3\eta]\boldsymbol{\gamma}}{\boldsymbol{L}+8\psi^3\eta\gamma} \tag{16}$$

$$d_p = (\boldsymbol{L} + 8\psi^3\eta\gamma) \begin{bmatrix} \left(\frac{\boldsymbol{\rho_p}}{\boldsymbol{\rho_t}}\right) \frac{\boldsymbol{\rho_t} {V_i}^2}{\sigma_e} \frac{\mathbf{1}}{\mathbf{2}\left[1+\beta\left(\frac{\rho_t}{\sigma_e}\right)^{0.5} V_i\right]} \\ + \frac{[(\mathbf{4}\psi-1)^{\mathbf{0.5}} - 8\psi^3\eta]\boldsymbol{\gamma}}{\boldsymbol{L}+8\psi^3\eta\gamma} \end{bmatrix} \tag{17}$$

3.3. Ballistic Test

The Ballistic or resistance to penetration tests were successfully done at the Nigerian Police Force (NPF) weapon divisional shooting ground at Uwani, Enugu, Nigeria. Six composite laminate armour sample plates of size 300mm by 400mm and thicknesses of 8mm, 12mm, 16mm, 20mm, 24mm and 28mm were targeted using two types of life bullets (Ogival and Conical nosed) of equal diameter and mass. The rifle used was the Beretta Cal 9 x 19 parabellum models 951 of muzzle velocity of 355m/s and the angle of attack was 0^0(normal). Figs. 2 to 7 show the ballistic impact, perforation and penetration on the six GFRP composite laminate samples.

Figure 2. Sample E, showing complete absorption of impact

Figure 3. Sample D, showing minimal shattering by impact

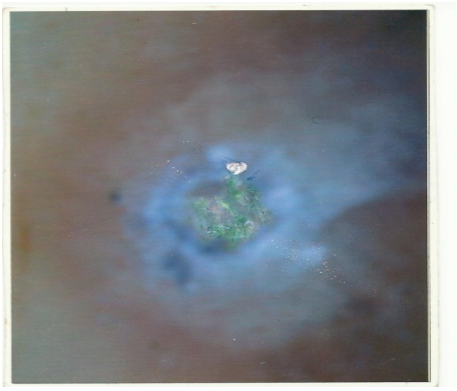

Figure 4. Sample C, showing some shattering and penetration, but no perforation

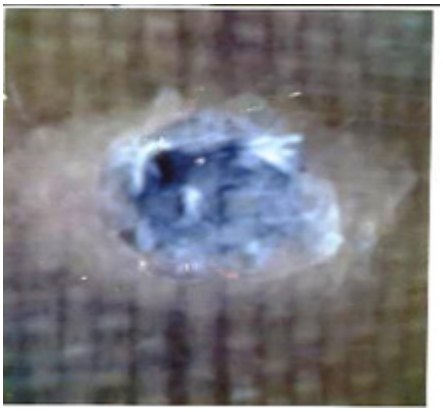

Figure 6. Sample A, showing heavy shattering but no perforation

Figure 5. Sample B, showing sign of penetration but no perforation

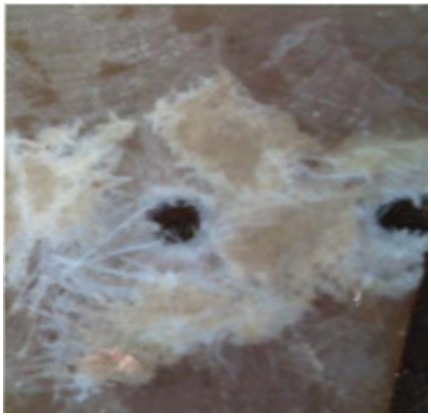

Figure 7. Sample F, showing failure with complete perforation

It was observed that five samples resisted or arrested the assault of the projectiles while the sixth sample failed (the bullets went through). The distance between the target and the gun was measured to be 50meters. After the ballistic experiment, the samples were examined. The Ultrasonic thickness measurement/Penetration and inspection was carried out on the six GFRP composite samples at BVL Nigeria Limited Port Harcourt, Rivers State, with Calibration Sensitivity Compression-Wave and Share-Wave Scanner. For composite analyzer probe of procedure ASTM E2580-07, the calibration was set at 200mm screen, while the sensitivity was set at 80% full screen height for 1.5mm hole from the calibration block. Scanning and transfer loss reduction values are as indicated in Table 5.

From Tables 9 and 11, it is observed that the tensile strength of the material before ballistic deformation was 145.833MPa and 97.3MPa after ballistic deformation.

Table 5. Ultrasonic Thickness Measurement/Penetration Inspection Result

SAMPLE	TYPE OF PROJECTILE USED	ORIGINAL THICKNESS (mm)	MEASURED THICKNESS (mm)	PENETRATION OR REDUCTION (mm)	TYPE OF TEST
E	Conical	28	10	18	PEN. TEST
	Ogival	28	12	16	PEN. TEST
D	Conical	24	7	17	PEN. TEST
	Ogival	24	8.5	15.5	PEN. TEST
C	Conical	20	4	16	PEN. TEST
	Ogival	20	6	14	PEN. TEST
B	Conical	16	2.5	13.5	PEN. TEST
	Ogival	16	4	12	PEN. TEST
A	Conical	12	1	11	PEN. TEST
	Ogival	12	2	10	PEN. TEST
F	Conical	8	0	8	PEN. TEST
	Ogival	8	0	8	PEN. TEST

Table 6. Impact Test Analysis before Ballistic Deformation

S/No	MATERIAL SAMPLES	No OF ITEM TESTED	IMPACT FORCE (N)	IMPACT VALUES (J)	MEAN IMPACT VALUES (J)
1	E	A	24	53.71	50.279
		B	26	52.72	
		C	28	51.70	
		D	28.7	51.33	
		E	32	50.80	
		F	34.6	49.34	
		G	36	48.86	
		H	36	48.86	
		I	38.7	48.06	
		J	40	47.41	
2	D	A	40	47.82	46.354
		B	42	46.83	
		C	42.6	46.83	
		D	41.5	47.33	
		E	42.5	48.58	
		F	44	46.41	
		G	44.5	46.16	
		H	46	45.74	
		I	50	44.27	
		J	52	43.57	
3	C	A	64	39.46	37.589
		B	62	40.30	
		C	64.5	39.27	
		D	64	39.74	
		E	85	34.21	
		F	72	36.88	
		G	74	36.39	
		H	72	36.97	
		I	70	37.26	
		J	78	35.41	
4	B	A	82	33.41	32.764
		B	78	34.41	
		C	86	32.39	
		D	86.7	32.19	
		E	80	34.43	
		F	84	33.20	
		G	88.2	31.37	
		H	84	33.20	
		I	86.5	31.88	
		J	90	31.16	
5	A	A	94.5	28.45	30.1
		B	106	25.03	
		C	102	26.64	
		D	102	26.64	
		E	114	22.85	
		F	116	22.30	
		G	102	26.43	
		H	108	25.03	
		I	112	23.51	
		J	108	24.49	

Table 7. Impact Test Analysis after Ballistic Deformation

SN	MATERIAL SAMPLES	NO OF ITEM TESTED	IMPACT VALUES (J)	MEAN IMPACT VALUES (J)
1	A	A	20.0	16.8
		B	10.0	
		C	24.0	
		D	16.0	
		E	14.0	
2	B	A	28.0	31.6
		B	20.0	
		C	32.0	
		D	52.0	
		E	26.0	
3	C	A	28.0	30.0
		B	38.0	
		C	34.0	
		D	26.0	
		E	24.0	
4	D	A	42.0	36.0
		B	36.0	
		C	40.0	
		D	34.0	
		E	28.0	
5	E	A	48.0	48.0
		B	56.0	
		C	64.0	
		D	32.0	
		E	40.0	

Table 8. Tensile Test of Composite Sample before Ballistic Deformation (Load/Extension)

A		B		C		D		E	
Load (N)	**Extension (mm)**	**Load (N)**	**Extension (mm)**	**Load (N)**	**Extension (mm)**	**Load (N)**	**Extension (mm)**	**Load (N)**	**Extension (mm)**
0	0	0	0	0	0	0	0	0	0
1605	1.825	1480	1.425	1420	1.788	1370	1.563	1485	1.575
2570	3.613	2740	3.438	2830	4.05	2325	3.513	2830	3.725
3515	5.613	4465	5.575	4345	5.8	3345	5.238	4260	5.463
4170	7.138	6015	7	5825	7.413	4580	6.775	5630	6.813
		7640	8.588	7145	9.388	5575	8.135	6980	8.225
		8915	9.95	8520	11.413	5963	9.078	7867	9.431
		9458	12.417	9250	12.847	6363	9.875	8350	10.4
		9863	14.094	9831	14.219	6950	10.25	8750	12

Table 9. Tensile Test of Composite Sample before Ballistic Deformation (Stress/Strain)

A		B		C		D		E	
Stress (MPa)	**Strain**	**Stress (MPa)**	**Strain**	**Stress (MPa)**	**Strain**	**Stress (MPa)**	**Strain**	**Stress (MPa)**	**Strain**
0	0	0	0	0	0	0	0	0	0
40.125	0.0114	14.8	0.0089	17.75	0.0112	27.4	0.0098	24.75	0.0098
64.25	0.0226	27.4	0.0215	35.375	0.0253	46.5	0.022	47.167	0.0233
87.875	0.0351	44.65	0.0348	54.313	0.0363	66.9	0.0327	71.0	0.0341
104.25	0.0446	60.15	0.0438	72.813	0.0463	91.6	0.0423	93.833	0.0426
		76.4	0.0537	89.313	0.0587	111.5	0.0508	116.333	0.0514
		89.15	0.0622	106.5	0.0713	119.26	0.0567	131.117	0.0589
		94.58	0.0776	115.625	0.0803	127.26	0.0617	139.167	0.065
		98.63	0.0881	122.888	0.0889	139.0	0.0641	**145.833**	0.075

Table 10. Tensile Test of Composite Sample after Ballistic Deformation (Load/Extension)

A		B		C		D		E	
Load (N)	**Extension (mm)**	**Load (N)**	**Extension (mm)**	**Load (N)**	**Extension (mm)**	**Load (N)**	**Extension (mm)**	**Load (N)**	**Extension (mm)**
1200	0.55	800	1.08	700	0.75	9000	0.17	800	1.2
2400	1.15	1600	1.35	1400	1.05	1800	0.24	1600	1.65
3600	1.55	2400	1.55	2100	1.3	2700	0.285	2400	2.25
4800	1.9	3200	1.75	2800	1.6	3600	0.335	3200	2.65
6000	2.2	4000	1.95	3500	1.85	4500	0.375	4000	3.05
7200	2.45	4800	2.16	4200	2.15	5400	0.425	4800	3.4
		5600	2.3	4900	2.55	6300	0.47	5600	3.75
		6400	2.5	5600	3.0	7200	0.515	6400	4.25
		7200	2.75	6090	3.4	8100	0.58	7200	4.7

Table 11. Tensile Test of Composite Sample after Ballistic Deformation (Stress/Strain)

A		B		C		D		E	
Stress (MPa)	**Strain**	**Stress (MPa)**	**Strain**	**Stress (MPa)**	**Strain**	**Stress (MPa)**	**Strain**	**Stress (MPa)**	**Strain**
2.632	0.00183	7.407	0.0036	9.09	0.0025	9.868	0.00567	10.81	0.004
5.263	0.00383	14.815	0.0045	18.182	0.0035	19.737	0.008	21.62	0.0055
7.895	0.00517	22.222	0.0052	27.273	0.00433	29.605	0.0095	32.43	0.0075
10.53	0.00633	29.63	0.0058	36.364	0.00533	39.474	0.0112	43.24	0.00883
13.16	0.0073	37.037	0.0065	45.455	0.00617	49.342	0.0125	54.05	0.0102
15.79	0.00817	44.444	0.0072	54.545	0.00717	59.211	0.0142	64.86	0.0113
		51.852	0.0077	63.636	0.0085	69.079	0.0157	75.68	0.0125
		59.259	0.0083	72.727	0.01	78.95	0.0172	86.49	0.0142
		66.667	0.0092	79.1	0.0113	88.816	0.0193	**97.3**	0.0157

4. Experimental Results and Discussion

4.1 Impact (Ballistic) Test Results

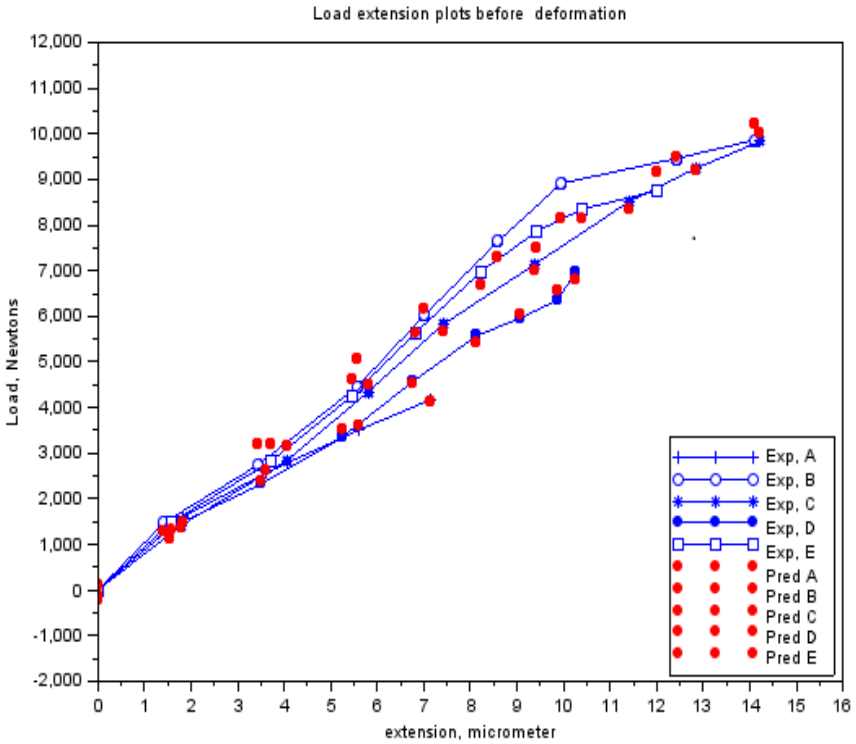

(a): Load-Extension plots (experimental and predicted) before ballistic deformation

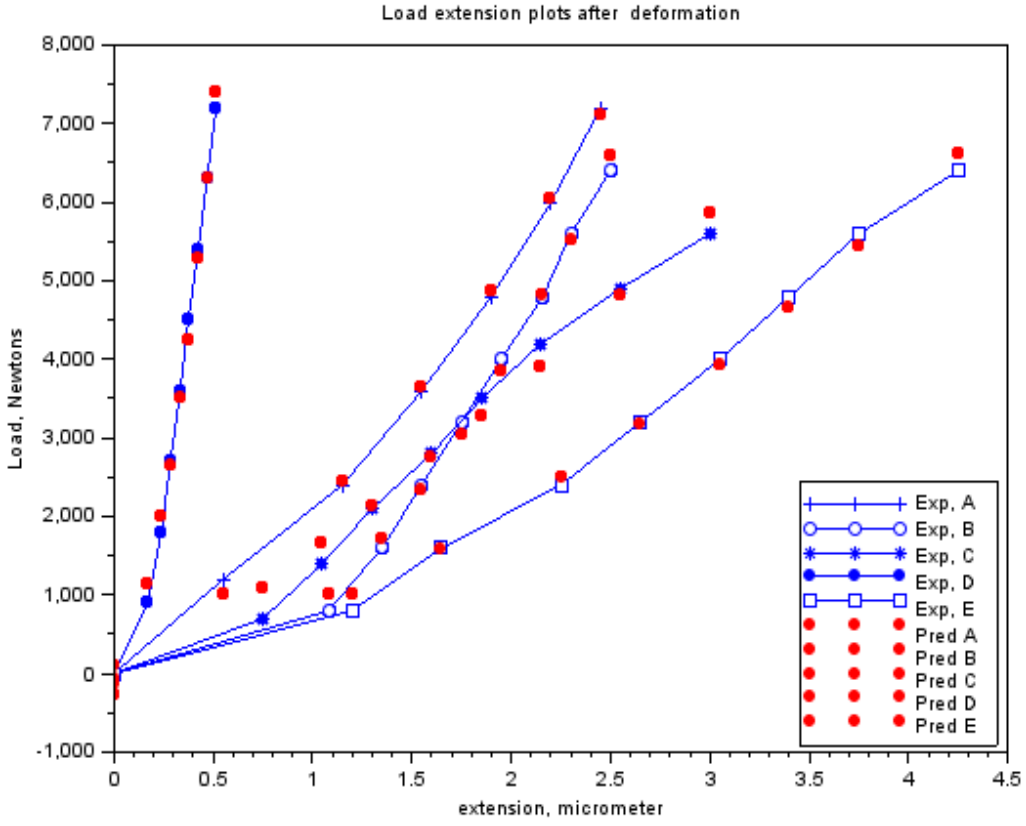

(b): Load-Extension plots (experimental and predicted) after ballistic deformation

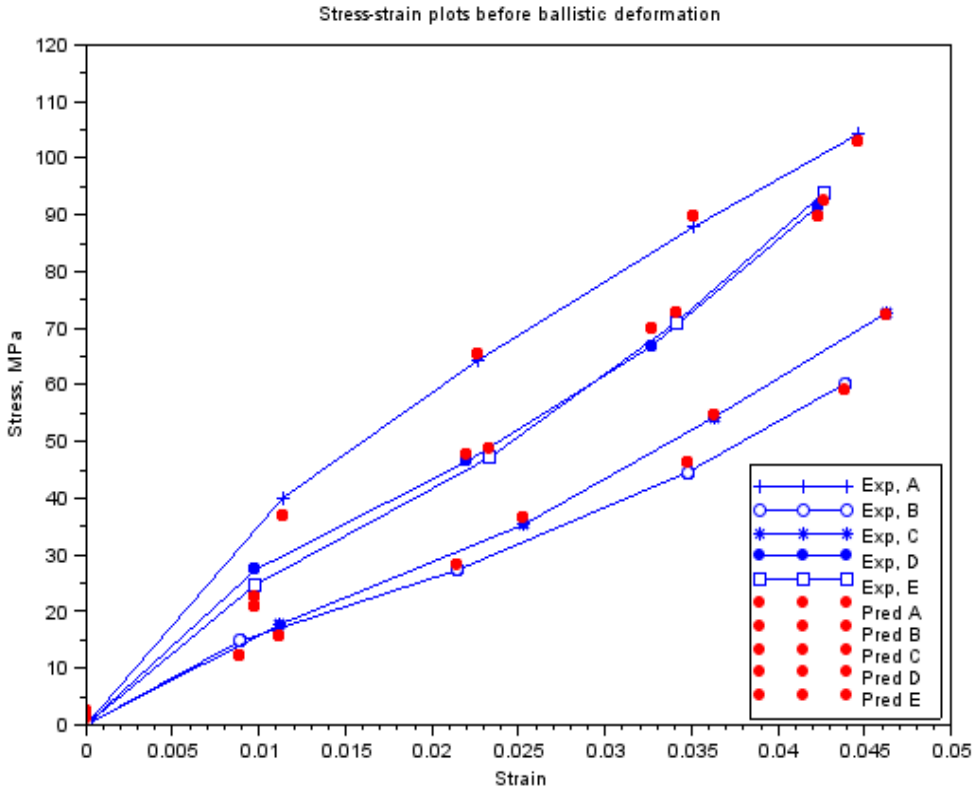

(c): Stress-Strain plots (experimental and predicted) before ballistic deformation

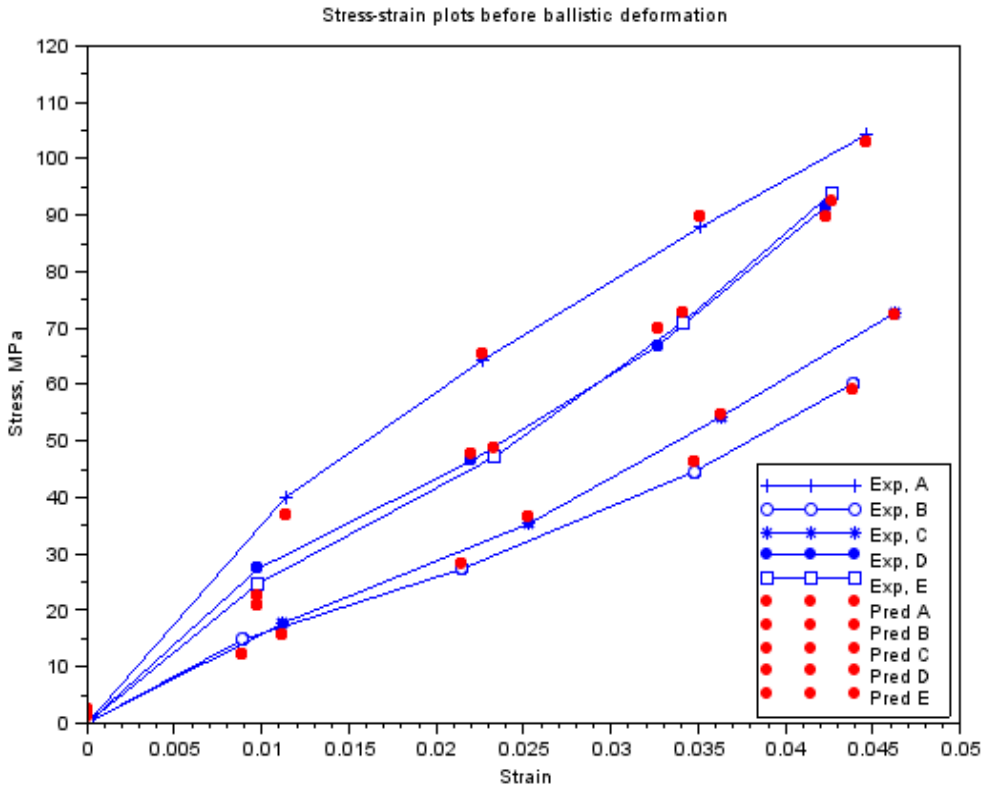

(d): Stress-Strain plots (experimental and predicted) after ballistic deformation

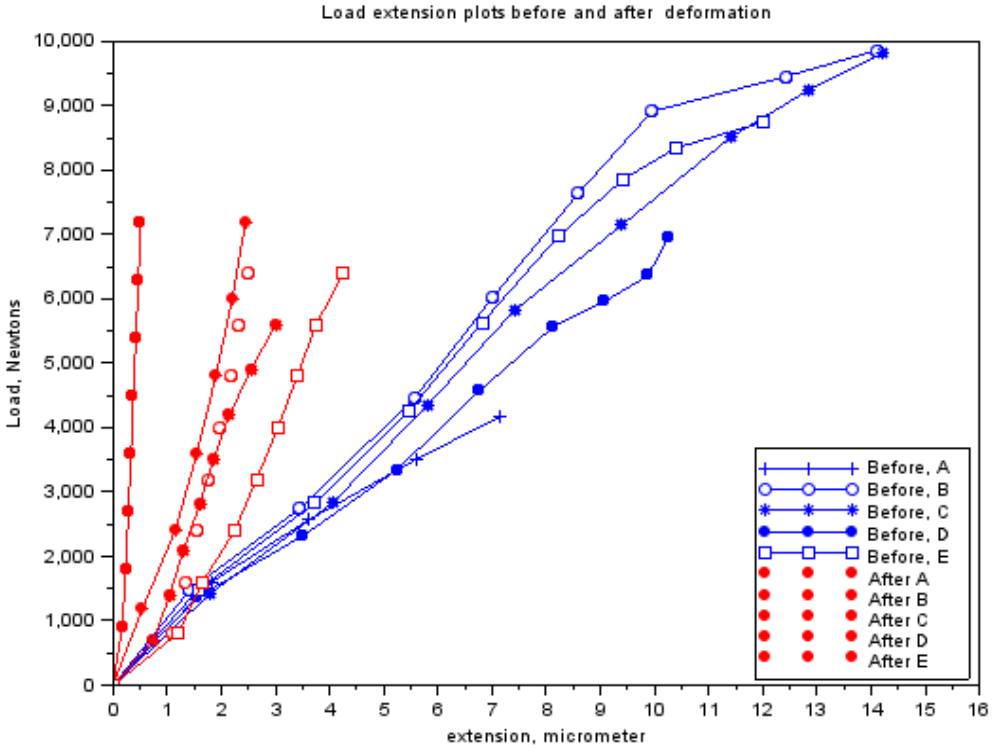

(e): Load-Extension before and after ballistic deformation

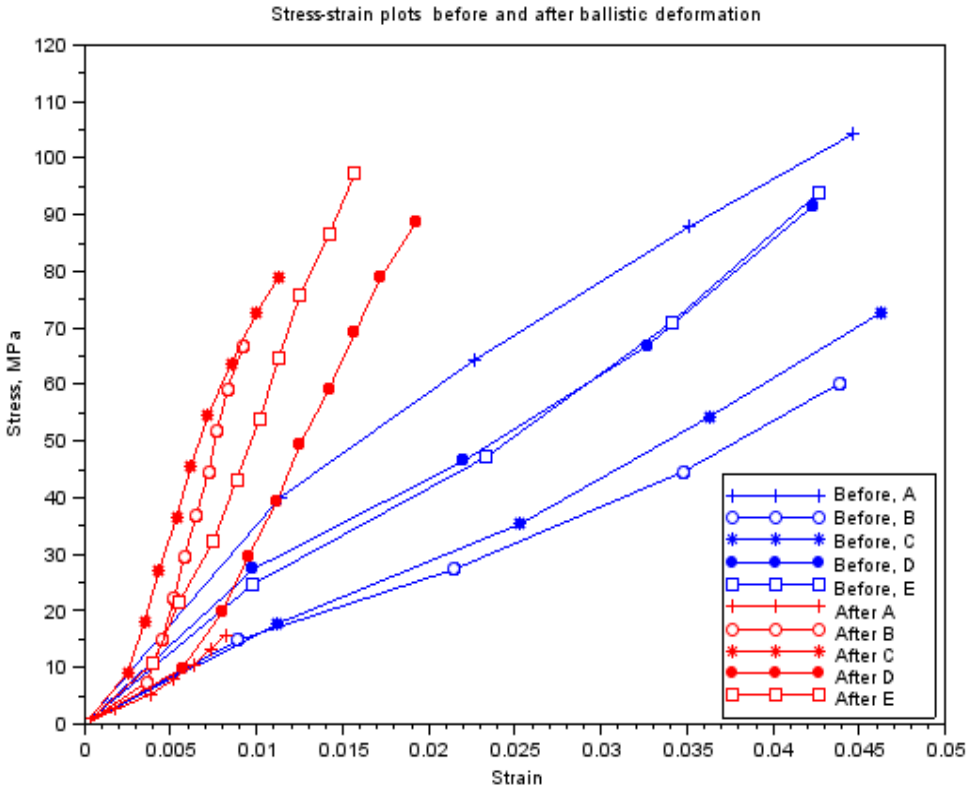

(f): Stress-Strain plots before and after ballistic deformation.

Figure 8. Various responses of the GRP laminate samples before and after ballistic deformation

Fig 5.5 shows the various responses of the composite samples before and after ballistic deformation. It was observed from Fig 5.5, (e) and (f) that before ballistic deformation, the composite samples were elastic. The extension and strain were of significant values. But after deformation, the material became less elastic, and the extension and strain were of little value. The legends in Figs. 8 (a), (b), (c), and (d) show that the red coloured dots indicate predictions while the blue lines indicate experimental plots. The data and the plots obtained from the impact (ballistic) and tensile tests on samples were statistically verified. The plots (Figs. 8a to 8f) took the form of a quadratic curve that yields the following model;

$$y = a + bx + cx^2 \tag{18}$$

The coefficients a, b, c and the corresponding coefficient of determination '$R^{2'}$ are shown in Tables 12 to 15.

The values of coefficient of determination R^2 in the tables above for all plots were approximately equal to unity. That indicates a good agreement with the experimental data.

Table 12. Statistics of Tested Data for Load/Extension before Ballistic Deformation

Material Samples	Constants			Coefficients of Determination (R^2)
	a	b	c	
A	55.6443	851.5130	-39.5219	0.9973
B	-225.6861	1081.8682	-24.2055	0.9856
C	-128.3863	854.6220	-9.8992	0.9973
D	116.7900	645.6050	0.6409	0.9958
E	-112.7420	939.7622	-13.9491	0.9911

Table 13. Statistics of Tested Data for Load/Extension after Ballistic Deformation

Material Samples	Constants			Coefficients of Determination (R^2)
	a	b	c	
A	98.4991	1295.5077	639.3145	0.9984
B	-58.5949	-279.4041	1174.1209	0.9962
C	-260.0118	1698.8884	113.0572	0.9836
D	-115.8399	3728.6423	21103.562	0.9952
E	-102.0688	663.5712	216.4704	0.9957

Table 14. Statistics of Tested Data for Stress-Strain before Ballistic Deformation

Material Samples	Constants			Coefficients of Determination (R^2)
	a	b	c	
A	1.4052	3402.8684	-25229.067	0.9972
B	1.4511	1167.9351	3388.6612	0.9941
C	0.8854	1255.9838	6208.3558	0.9980
D	2.3704	2065.8198	-23.6914	0.9914
E	1.8873	1881.1624	5740.8756	0.9952

Table 15. Statistics of Tested Data for Stress-Strain after Ballistic Deformation

Material Samples	Constants			Coefficients of Determination (R^2)
	a	b	c	
A	0.2153	852.7472	126614.19	0.9985
B	-1.2833	385.3469	807923.18	0.9900
C	-4.5502	7646.175	5008.2114	0.9830
D	-2.5143	1971.9229	155164.34	0.9905
E	-2.4418	3412.6092	201345.98	0.9936

5. Conclusions

This work shows that one of the governing factors in the damage resistance is the nose shape of the impacting projectile. Here the performance of the laminates could be properly tailored by controlling the strength parameters for the design against failure. It has also shown that great strides can be achieved in the production and testing (static and ballistic) of the armour protecting hand lay-up GFRP composite laminate plates. This work has also shown that; despite all odds, the hand lay-up composite armour developed, proved considerable strength of 145.83 MPa before ballistic deformation and 97.3 MPa after ballistic deformation. The ballistic limit or critical velocity can be successfully predicted for any thickness of the armour protecting body (GFRP laminate samples) produced. Finally, the data obtained from the experimental tests (tensile and impact) resulted to the plots of Fig. 8 which yielded the mathematical model of equation (18), the coefficients of this model were statistically analyzed and the resulting coefficients of determination are approximately unity an indication of good relationship (conformity) the between experimental and analytical results. Also, the result of Table 5 shows that Sample E actually gives the best impact absorption.

REFERENCES

[1] Cantwell, W.J. & Morton, J. (1989). Comparison of Low Velocity & High Velocity Impact Response of CERP Composites, 20, 545–51.

[2] Prewo, K.M. (1980). The Importance of Fibres in Achieving Impact Tolerant Composites. Phil. Trans. R. Soc. London, A 294, 551 – 58.

[3] Babaniyi, Babatope. (2000). Self-reinforcing Polymeric Composite Materials in Ballistic Protection. Technical Conference of the Polymer Institute of Nigeria. November 22 and 25.

[4] Morh, J. G., et at.,(1973) SPI Handbook of Technology & Engineering of Reinforced Plastics/Composites, 2nd Edition, New York, Van Nostrand Reinhold Company.

[5] Frados, J., (1976). SPI Plastics Engineering Handbook, Society of the Plastics Industry, Inc., 4th Edition, New York, Van- Nostrand Reinhold Company.

[6] Agrannoff, J., Editor, (1975). Modern Plastics Encyclopedia, Vol. 52 (10A), New York, McGraw-Hill, Inc.

[7] Skeist, I., (1966) Editor, Plastics in Building, New York, Reinhold Publishing Corp.

[8] Randolph, A. F., (1960) Editor, Plastics Engineering Handbook of the Society of Plastics Industry, Inc., New York, Van Nostrand Reinhold Company.

[9] Richard Wood (1980). Car Body in Glass Reinforced Plastic. Pentech Press Limited, London, pp 43 - 45.

[10] Enetanya, A. N; (1998) Fibre Reinforced Composite for the Aircraft & Automobiles Industries. Nigerian Society of Engineers' Technical Session. April. pp. 60-73.

[11] Edelugo, S. O. (2000). Damage Evaluation & Reinforcements, Combination in the Development of GRP Automobile body Work. Ph.D. Thesis, University of Nigeria, Nsukka. pp 1-300.

[12] Ihueze, C. C. (2005). Optimum Buckling Model of GRP Composites; Ph.D. thesis, University of Nigeria, Nsukka.

[13] Miller, L. & Xu, H. (1991). On the pseudo-elastic hysteresis, Acta Metallurgy Materials, Vol. 39, pp 263-271.

[14] Falk, F. (1980) Model free Energy, Mechanics & thermodynamics of shape memory alloys, Acta Metallurgical, Vol. 28, pp. 1773-1780.

[15] Berholf, L.D., and Benzley, S.E. (1968). "TOODY II, A Computer Program for Two-Dimensional Wave Propagation," SC-RR-68-41, Sandia Laboratories, Alburquerque, New Mexico, November .

[16] Hageman, L.J., and Walsh, J.M. (1971). "HELP, A Multi-Material Eulerian Program for Compressible Fluid & Elastic-Plastic Flows in Two Space Dimensions and Time," Vol. 1, BRL CR 39, Systems, Science, and Software, LA Jolla, Calif.

[17] Wilkins, M.L., French, M.L., French, S.J., & Sorem, M. (1970). "Finite-Difference Scheme for Calculating Problems in Three Space Dimensions & Time," Proceedings of International Conference on Numerical Methods in Fluid Dimensions – II, Berkeley, California, pp. 30 – 33.

[18] Johnson, G.R. (1976). "Analysis of Elastic-Plastic Impact Involving Severe Distortions", Journal Of Applied Mechanics, Vol. 43, No. 3, TRANS. ASME, Vol. 98, Series E, Sept. pp. 439 – 444.

[19] Zienkiewicz, O.C., (1971) the Finite-Element Method in Engineering Science, McGraw-Hill, New York, N.Y.

[20] Abrate, S. (1994). Impact on Laminated Composites: Recent Advances. Applied Mech. Rev., 4711 pp. 517-544.

[21] Cantwell, W.J. & Morton, J. (1991). The Impact Resistance of Composite Materials: A Review Composites, 22, 347 – 362.

[22] Kumar, K. Siva and Bhat, T. Blakrishna. (1998) Response of Composite Laminates on Impact of High Velocity. Key Engineering Materials. Vol. 141-143, Pp 337-348.

[23] Wen, H.M. (2001) Penetration and Perforation of thick FRP laminate. Composites Science and Technology, ELSEVIER, Vol. 61, Pp. 1163 – 1172.

[24] He, T., Wen,H.M; Qin, Y, (2007) Penetration and Perforation of FRP Laminates Struct transversely by Conical-nosed projectiles. Composite Structures, ELSEVIER, Vol. 81, Pp. 243-252.

[25] Wen, H.M. (2000). Predicting the Penetration & Perforation of FRP Laminates Struct Normally by Projectiles with Different Nose Shapes. Composite Structures, 49, 321 –329.

[26] Zhu, G., Goldsmith, W., and Dharan, C.K.H. (1991). Penetra tion of Laminated Kevlar by Projectiles – I Experimental Investigation. Int. J. Solids Structure, 29, 399-420.

[27] Abdullah, M.R; Cantwell, W.J. (2006) The impact resistance of fibre-metal laminates based on glass fibre reinforced polypropylene. Polymer Composites. Vol. 27, No. 6, Pp 700 – 708.

[28] Ben-Dor, G., Dubinsky, A. and Elperin, T., (2002) "Optimization of the nose shape of an impactor against a semi-infinite FRP laminates", Composites Science and Technology, Vol. 62, No. 5, Pp. 663 – 667.

[29] Cartridges of the World (.22 caliber). http://www.wikipedia. com/.22 short.

[30] Wen, H.M; Reddy, T.Y., Reid, S.R and Soden, P.D. (1998). Indentation, Penetration, & Perforation of Composite Laminates & Sandwich Panels under quasi-static & projectile loading. Key Engineering Material, 141-143, 501-52.